Tumor Region detection in MRI Images using Novel Kernalized Fuzzy C-Means Clustering Algorithm

P.Gangadhara Reddy[1], T.Ramashri[2], K.Lokesh Krishna[3]

[12] Department of ECE, S.V.University College of Engineering, S.V.University, Tirupati, A.P., India

[3]Department of ECE, S.V.College of Engineering, Tirupati, A.P., India

[1]gangadharareddy.p@gmail.com

Abstract: In medical diagnosis, brain tumor identification and evaluation is important. The proposed study focuses on segmenting anomalies in MR DICOM axial brain slices, since that format has the advantage of preserving broad metadata. A semi-automatic device has been built in the sense of a DICOM analysis to both usual and abnormal structures for each MR slice. In this paper, we suggest an algorithm for identification of human brain tumors in Magnetic Resonance Imaging (MRI) that contains a Kernel Fuzzy C-Means (KFCM). This procedure mainly removes the color, texture and place characteristics of each pixel by choosing the required color space depending on the grey image strength. Secondly, updated membership will be calculated using a fuzzy C-means (FCM) Algorithm and, final, the kernel FCM clustering algorithm is used to detect the tumors location by updating its membership function obtained on the basis of the various features of tumor image. The simulation results demonstrate that the algorithm proposed is able to better detect abnormal and normal tissue with less grey strength detachment in the human brain.

Index Terms: DICOM processing, Feature extraction, Fuzzy clustering, Gray level intensity, MR brain segmentation, Region Description.

I. INTRODUCTION

Digital image processing (DIP) is an emerging field of biological science such as tumor identification, recognition, disease detection and essential parts of the human body. The automated detection of tumors is an important aspect of the medical sciences [1]. The human body consists of multiple cell types of which the brain performs quite a important role. The brain is the most essential part of nervous system [2]. In comparison, it is the central nervous human system kernel.

Increased diagnostic significance is provided by standard Digital Imaging and Medical Communications (DICOM) image formats. MR imaging systems that cooperate with DICOM conform to a particular standard on digital medical image archiving and correspondence. DICOM (.dcm) files contain metadata, such as patient analysis and measurements. A regular number of tags is grouped into the DICOM header object. These are grouped into categories, the image plane, MR/CT image and patient information including image pixels [3,4]. These are listed as patient information. Based on data elements across each class, the size of this header varies. For instance: the picture plane system takes several key parameters including slice location, slice position and pixel distance. The spatial relation between the slices is determined from these parameters. DICOM enables the development of private tags that identify open data elements in the created application. Different imagery modes store DICOM digital files, and have higher amounts of metadata than other formats. DICOM offers harmonization, which thoroughly analyses the research patient and is compatible with several trade tools [5].

The abnormal growth of the tissue can interrupt the proper function of brain. It indicates that the detection of brain tumors at advanced stages is very important to saving lives [6]. Though, very high speed and precision can be used for tumor detection processes. This can only be achieved by the use of MR images and suspect regions are extracted from complicated medical images through MR image segmentation. The typical flow diagram of MR image segmentation are shown in Fig. 1. Experts manually perform the detection of a brain tumor. However, in some problems, they take a lot of time and various experts can

vary greatly in their segmentation of the MR image [7]. For these purposes it is increasingly important to automatically detect brain tumors. Automatic brain tumor detection may enhance tumor survival risk. There is no specific procedure for brain tumor detection in the medical community [8].
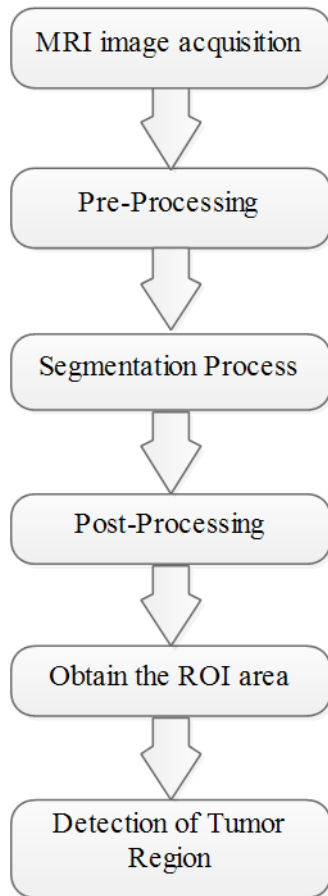
Fig. 1. Typical flow diagram of MRI segmentation

Detection of brain tumors ensures that not only the infected area of the brain is known, but also the shape, scale, border and location of the tumor. For imaging the brain, various imaging methods like the MRI, computed tomography (CT), positron emission tomography (PET) etc. are used. The MRI scan or CT scan will more commonly assess the brain tumor pathology. Though, the CT scan might produce radiation which is dangerous to the human body, while the anatomic tissue formation of the brain is specifically visualized by MRI [9]. MRI is a tool for the development of accurate photographs of organ and tissues by means of a magnetic field and a radio wave. Researchers are actively scrutinizing and allowing MR images incredibly complex, so that pathologists can obtain a greater background in diagnosing patients [10].

This paper outlines the main contributions:

- The benefit of this research analysis is the Kernelized fuzzy(image-enhancing) clustering strategy that efficiently decreases the field of focus of the brain segments.
- We used DICOM's attributes, such as the patient in image position, pixel distance and image orientation, as key to the generation of brain structures model and volumetric study, for each brain slice in this work.
- The fuzzy clustering is used for improving the image in the identifying of the objects of concern by correctly choosing the 'k' number of clusters. Building on the silhouette metric, the necessary k is selected between 2 and 9 clusters (k).
- The proposed study is initiated with an image consistency, similarity, and statistical tests. The method is also checked and verified against expert data on the clinical MR brain sequence.

II. PREVIOUS RELATED WORKS

Magnetic resonance imaging is used for detection and visualization of the internal structure of the human body in the medical field. It is primarily used to find variations in the tissues in the body and are slightly greater than the CT scan. This method is also well suitable for the diagnosis of brain tumors and cancer imaging. In general, CT utilizes ionizing radiation in contrast while MRI uses the powerful magnetic field to align nuclear magnetization which results in changes to the radio frequency alignment observable by the scanner. An image based tumor identification analysis is given in this article [11,12]. The technique of CT scan is used for photographs of the injured brain area. The images of the CT scans have been seen in gray-sized pictures because the CT scan system embraces this color type and promotes the tumor's image identification. Any brain clotting that indicates damage of any type can be observed in color as dark grey. The method of extracting parameters is simply like gathering and plotting information per pixel [13]. The images from CT scan show that a white and brain-damaged cell tumor is seen in black color, so binary pixel sizes showing the brain-damaged cells to 0 and shows a tumor to 1, so further analyses such as MATLAB tests and charts can be conducted by the extraction process. This procedure will separate the patient with a damaged brain from the normal patient. The tumor can also be clearly detected based on the image [14]. We also used k-means, c-fuzzy clustering and other segmentation techniques in this article.

Fuzzy C-means is a soft clustering where each pixel will belong to two or more cluster memberships. The Description of distances from cluster centers to models identify the targets [15]. Although only image strength values are taken into consideration, it offers high noise and enhanced standard of segmentation [16]. A K-means and FCM algorithm is given, in which K-means initially segmentation, FCM further segment on

the image and an FCM technique detects an approximate segmented tumor by exact selection of the cluster [17]. The traditional FCM is restricted to noise sensitivity, while in K it is clustered. However, before segmentation the threshold should be fine, as the complex structure of the brain is very difficult [18].

III. PROPOSED APPROACH

This section describes an idea employed by the proposed technology. There are mainly six modules available for the proposed system: image acquisition, pre-processing, segmenting, post-processing, extraction of features, stage detection. Filtering is done on the MR image during preprocessing. In separate segmentation work, K-means, Fuzzy C-means and Kernalized Fuzzy C-mean algorithms are used [19]. For function extraction, thresholding is used. In this work, two different datasets of brain slices were used. First, the KAGGLE dataset contains 22 brain MR DICOM slices. Secondly, to evaluate the performance of the proposed model, the ZENODO data set has been used. In addition, ten patients with approximately 200 brain parts have been acquired in the Zenodo dataset in this work. The proposed solution to the segmenting and study of MR DICOM slice is set out in this section. Initially, pre-processing of DICOM slices is feasible. Segmentation of DICOM slices preprocessed is subject to fuzzy clustering for the improvement of the image. The silhouette metric is used to select the right clusters and the enhancement by morphological procedures of derived structures. The ROI is then collected by image post-processing techniques like MCW, RG and DRLS and checked using resemblance tests. Then the tumor is extracted. Fig. 2 illustrates the complete architecture.

A. MRI image acquisition:

1) Data collection: MRI input images from the various open access web research libraries in DICOM, MHA and JPEG formats have been obtained.
2) Conversion of the file format: Most of the images that were obtained were in DCM format. We have used the programmed tool for the. DICOM image.
3) Normalization of Size: Variable sized images have been acquired from multiple sources; thus both pictures are scaled to (255 * 255) pixels normalized.

B. Image pre-processin:

1). Remove color components for Fuzzy C-means and K-means by changing to grey mode
2). Improve image consistency with a medium filter.
3). Chart the histogram for amplitude distribution studying and analyzing of the pixels.

4). Adjustment of intensity if necessary.
5). Equalization of histogram
6). This section formats the image.

C. Segmentation:

This article contrasts three major segmentation approaches focused on clusters called KFCM, Fuzzy C-Means and K-Means. When a group is clustered, unlabeled pattern sectors are separated or grouped into a few clusters such as the related patterns. These classes are referred to as clusters.

3.1 K-Means Clustering Algorithm

K-means is an unsupervised clustering algorithm. This gives a very simple way to classify a certain number of clusters, i.e. a group of data like into K clusters. The key idea for this algorithm is to set K centers for each group [20]. One for each group, randomly select the K cluster centers. Distance measurement plays a key role in the performance of this algorithm. Multiple distance measuring techniques like Euclidean, Manhattan and Chebychev etc. are available for this algorithm. We can use Euclidean as a metric distance, since it is fast, robust and easy to comprehensive. The classic K-means algorithm is described step-by-step [21] as follows:

Algorithm-1:K-means clustering algorithm

Assume that, $A = a_1, a_2, a_3, \ldots..a_n$ be the set of data points and $C = c_1, c_2, c_3, \ldots..c_n$ be the set of centers.

1: Define 'K' cluster number.
2: Identifying cluster 'c' spontaneously.
3: Measure the distance from the cluster centre and data point.
4: Data point assigned for the cluster with a minimum distance from the cluster centre and assign all data points to the closest cluster centres.
5: The following is re-calculation of the cluster centre.

$$X_n = \frac{1}{c_n} \sum_{m=1}^{c_n} A_n \qquad (1)$$

where 'c_n' is the n-th cluster number of data points.
6: Recalculating the distance from each newly acquired cluster cenre to each data point.
7: If no reassigned data points then stop, otherwise repeat steps 3 to6.

The Euclidean distance is determined from each pixel to each centre of the cluster. In distance calculation all pixels are separately compared to all cluster centers. The pixel contributes to a cluster that is shorter across both. The core is then replenished. Each pixel is then compared again for all centers [22]. This method continues until the centre converges, with a cumulative number of iterations testing the convergence. The

clustering efficiency of that algorithm is optimized several times with a different initialization by repeating K-means to classify
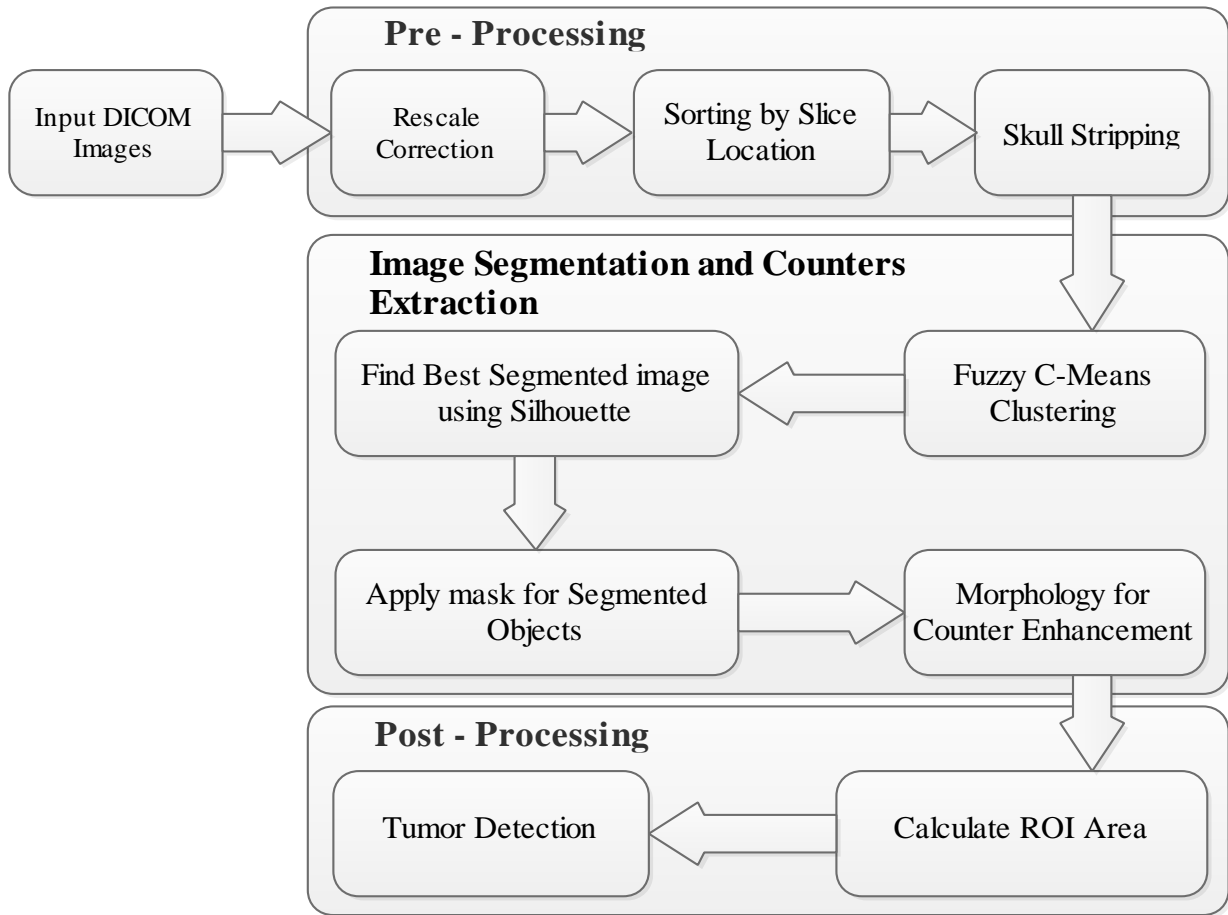
Fig. 2. Proposed MRI DICOM images Tumor detection

best centroids. It improves machine performance and facilitates multi-dimensional vectors. This algorithm is then programmed to decrease an objective parameter known as the squared error function:

$$X_n = \sum_{n=1}^{c} \sum_{m=1}^{c_m} (\|a_n - c_m\|)^2 \qquad (2)$$

Where $\|a_n - c_m\|$, is the Euclidean distance between a_n and C_m, the c_n is the number of n-th cluster data points and the c is the number of cluster centers

3.2 Fuzzy C-Means Clustering Algorithm:

Bezdek introduces the FCM clustering algorithm, here each data pixel belongs to two or more clusters. A much closer the data to the cluster centre is to the particular cluster hub [23, 24], the more its membership is. The objective function of the fluid-specific P cluster centroids Q is to be reduced.

$$S_i(P,Q) = \sum_{n=1}^{N} \sum_{m=1}^{C} (p_{mn})^i (\|a_n - c_m\|)^2 ; \quad 1 \le i \le \infty$$

$$(3)$$

Where $A = a_1, a_2, a_3, \ldots a_n$ is an Equation (3) $X \times N$ data matrix and i is any real number that is greater than 1. X, N and C represent the dimension of each a_i vector, the number of vectors (image pixel numbers), and the cluster number. $P_{mn} \subseteq P(X \times N \times C)$ is called vector an n-th cluster membership, which is consistent with $P_{mn} \epsilon [0 \ 1]$ and $\sum_{P_{mn}} = 1$, $n = 1,2,3,\ldots,N$. The membership function is as follows:

$$P_{mn} = \sum_{x=1}^{c} \left(\frac{(\|a_n - c_m\|)}{(\|a_n - c_x\|)} \right)^{\left(\frac{-2}{i-1} \right)} \qquad (4)$$

where $C = c_1, c_2, c_3, \ldots c_n$ is the matrix $A \times C$. The n-th cluster function centre is now determined as follows:

$$C_i = \frac{\sum_{n=1}^{N} (P_{mn})^i \times m}{\sum_{n=1}^{N} (P_{mn})i} \tag{5}$$

Where i is any individual number that exceeds 1, the level of fuzziness of the $d^2(a_n, c_m)$ is controlled. It is a similitude calculation between the two and is defined:

$$d^2(a_n, c_m) = \|a_n - c_m\|^2 \tag{6}$$

In this case, $\|\cdot\|$ can be defined as a straight Euclid or as a widely agreed distance like Mahalanobis. The MR image pixel intensity $X = k$ is indicated in the vector A. With the continuous P and C update, the FCM algorithm can optimize $S_i(P, Q)$, repeatedly until $\|(P_{mn})^{(k)} - (P_{mn})^{(k+1)}\| \leq \varepsilon$, $e = 0$ to 1, where k is the number of iterations. The classical fuzzy C-means clustering algorithm is seen as follows:

Algorithm-2:Fuzzy C-means clustering algorithm

The set of data points is $A = a_1, a_2, a_3, \ldots a_n$ and that the set of centers is $C = c_1, c_2, c_3, \ldots c_n$.

1: Fix cluster number c, $2 \leq c \leq m$. where m = data item number. Fix iwhere $1 < i < \infty$. Choose the any metric μ internal product caused.
2: Initialize $P(0)$.
3: In stage l, $l= 0, 1, 2\ldots$
4: Measure the Equation (4) Fuzzy Membership Function. P_{mn}
5: Then use equation (5) to calculate the fluidized centers C_i.
6: Repeat steps 2 and 3 to meet the minimum X or $\|(P_{mn})^{(k)} - (P_{mn})^{(k+1)}\| \leq \varepsilon$ value.

3.3 Proposed Kernelized fuzzy C-means clustering (KFCM)

The inner product algorithm can be implemented indirectly in space F. This trick can be used for clustering kernelized fuzzy C-means algorithms. The clustering centre, i.e. the clustering centers in functional space, is a common ground of these algorithms to represent the combined $\delta(a_n,)$sum of both [25, 26]. The objective function of the kernelized FCM algorithm is as follows:

$$X_n = \sum_{n=1}^{c} \sum_{m=1}^{N} (P_{mn})^i (\|\delta(a_n) - \delta(c_m)\|)^2 \tag{7}$$

Where δ is a nonlinear, implicit map as previously defined. Here δ (cm) is no longer represented as a linear cumulative value

among all δ (a_n) as such dual expression, but is still considered in the original space as a mapped point (image) of c_m, and with the kernel substitution trick we have:

$$\|d(a_n) - d(c_m)\|^2 = (d(a_n) - d(c_m))^T (d(a_n) - d(c_m))$$
$$= d^T(a_n) d(a_n) - d^T(a_n) d(c_m)$$
$$- d(a_n) d^T(c_m) + d^T(c_m) d(c_m)$$
$$= K(a_n, a_n) - 2K(a_n, c_m) + K(c_m, c_m)$$

In GRBF kernel $K(a,c) = e^{(-\|x-c\|^2/\sigma^2)}$, $K(a_n, a_n) = 1$
$K(c_m, c_m) = 1$, $d^T(a_n) d(c_m) - d(a_n) d^T(c_m)$
from equation (3) and (5) we get

$$X_i = 2 \sum_{n=1}^{C} \sum_{m=1}^{N} (P_{mn})^i (1 - K(a_n, c_m)) \tag{8}$$

The purpose of this paper is to evaluate the Kernel Fuzzy C-means (KFCM) validity criterion for MRI data sets. The GRBF kernel provides better segmentation findings in noise-corrupted images of simulated MRs than the dependent polynomial algorithms[27] was shown. We only look for the best index for the stable kernelized fuzzy C-mean clustering on the GRBF kernel. The objective function X_i in Equation (8) is identical to the FCM algorithm under P limitation can be reduced.

$$P_{mn} = \frac{\sum_{k=1}^{c} (1 - K(a_n, c_k))^{1/(i-1)}}{(1 - K(a_n, c_k))^{1/(i-1)}} \tag{9}$$

The centre of the cluster c_m of:

$$c_m = \frac{\sum_{m=1}^{N} (P_{mn})^i (K(a_n, c_m) a_n)}{\sum_{m=1}^{N} (P_{mn})^i K(a_n, c_m)} \tag{10}$$

Algorithm-3:Kernelized Fuzzy C-means clustering algorithm

Stage 1. For any positive constant, patch c, t_{max}, m >1 and ε>0.
Stage 2: $P_{mn}{}^0, C, x$ membership initialization.
Stage 3: In the case of. $t = 1, 2, \ldots, t_{max}$

(a) Upgrade the wholeprototype C_n^t with equation (10).

(b) Upgrading all memberships P_{mn}^t with equation (9).

(c) Evaluate $E^t = \max_{m,n} |P_{mn}^t - P_{mn}^{t-1}|$ to quit if;

$E^t \, \pounds \, e$

Finish

3.4 Improvement Morphological Operations

Masking of images can be used to denote the front, background. Contour-masking is important and distinguishes the objects from the original images.. The fuzzy method of clustering reveals the best segmented clusters. They shape a binary mask that overlay the individual parts to obtain the corresponding contour intensities. In order to ensure similarity, mutual information (M) is determined between a contour mask and the respective slice[28]. The weighted (H_i) addition to the initial slice(IS_i) of the contour mask (C_i) is:

$$H_i = \frac{1}{C_i} e^{-\frac{M_i - M_{min}}{M_{max} - M_{min}}} \qquad (11)$$

Where M_i represents C_i and OS_i mutual information. For the overall C_i, M_{max}, M_{min} is the most and least mutual information. A kind of contrast improvement strategy, mathematical morphology supports selectively enhancing the small diagnostic contour properties, overlaid on such a composite background. Dilation applies pixels to the slice contour edges. The method of dilation is carried out by:

$$C \, Å \, SE = \left\{ z \mid (\P E)_z \, Ç \, C^1 \; j \; \right\} (12)$$

where C is a binary mask pixel, SE is the structuring element, and then z is a reflected object. The whole process enhances the binary mask to prevent missing pixels across all directions, specifically at contour borders. Erosion is also carried out by equation 13,

$$CQSE = \left\{ \left\{ z \mid (SE)_z \, Í \; C \right\} \right\} \qquad (13)$$

The SE moves by specifying that z is limited to C. Erosion eliminates pixels and sharpens the boundaries of the object. Depending on the height of SE, the amount of pixels removed. Erosion strips the natural and irregular connected contours, which help to remove ROI efficiently at the post-processing levels.

3.5 Quantizing and Validating Tumors

High solidity ventricles and tumor area are used in the removed artifacts. The image-post-processing techniques are used to collect ROI from the brain structures to reduce the ROI from the removed objects. The tumor size is quantified by area and perimeter after determination of irregular areas. In order to determine the structural intersection of the Ground Truth (GT) including its clinical slices with the extracted ROI, validity metrics are used[29]. The segmentation procedure's output is validated by similarities like Dice, Jaccard, False Positive Rate

(FPR), and False Negatives Rate (FNRs). The statistical propagation of these steps is:

$$Jaccard(I_{gt}, I_{ROI}) = (I_{gt} \cap I_{ROI})/(I_{gt} \cup I_{ROI}) \quad (14)$$
$$Dice(I_{gt}, I_{ROI}) = 2(I_{gt} \cap I_{ROI})/(I_{gt} \cup I_{ROI}) \quad (15)$$
$$FPR(I_{gt}, I_{ROI}) = (I_{gt}/I_{ROI})/(I_{gt} \cup I_{ROI}) \quad (16)$$
$$1) \; FNR(I_{gt}, I_{ROI}) = (I_{ROI}/I_{gt})/(I_{gt} \cup I_{ROI}) \quad (17)$$

where, I_{gt} gives a segmented picture with the suggested technique to the ground truth and *IROI*.

3.6 Feature Extraction

It is still the procedure of getting more details about the shape, texture, color and contrast of an image. Texture interpretation is essentially an essential parameter of human visual perception and the framework of machine learning. Haralick et al.[30] implemented Gray Level Cooccurrence Matrix (GLCM) and texture function as one of the most frequently used image analysis applications. This procedure takes two steps to remove medical images from the functionalities. The first step is the GLCM calculation and the second is the estimation of the texture characteristics based on the GLCM.Highly dynamic nature, the retrieval of the related functionality is important throughout the brain MR images of diversified tissues like WM, GM and CSF. The identification and various stages of tumors (tumor stage) and therapeutic response evaluations could enhance textual outcomes and analyses. For some of the helpful features, the statistics form is given below:

(1) Contrast (C_{on}): In contrast, a pixel and its neighbor are measured in intensity over the image. Contrast is 0 for an image that is constant and defined as

$$Con = \sum_{i=0}^{x-1} \sum_{j=0}^{y-1} (i-j)^2 f(i,j) \qquad (18)$$

(2) Correlation (Cor): The correlation attribute defines the spatial dependency between the pixels. For a perfectly positive or negative picture, the correlation is 1 or -1. Correlation is NaN for a constant image.

$$cor = \frac{\sum_{i=0}^{x-1} \sum_{j=0}^{y-1} (ij) f(i,j) - M_i M_j}{\sigma_i \sigma_j} \qquad (19)$$

where M_i and S_i are the mean and standard deviation in the horizontal spatial domain and M_j and S_j are the mean and standard deviation in the vertical spatial domain.

(3) Energy (En): The quantifiable sum of pixels pair repeatments could be described as light. Energy. Energy is an image similitude calculation parameter. If the Haralicks GLCM

function defines energy, then it is also known as the second angular moment. Energy is 1 and is defined as a continuous image

$$En = \sqrt{\sum_{i=0}^{x-1} \sum_{j=0}^{y-1} f^2(i,j)} \qquad (20)$$

(4) Homogeneity (Hg): Returns a value that calculates the similarity to the GLCM diagonal of the distribution of components. Homogeneity 1 is defined for a diagonal GLCM

$$Hg = \sqrt{\sum_{i=0}^{x-1} \sum_{j=0}^{y-1} \frac{f(i,j)}{1+|i-j|}} \qquad (21)$$

3.7: Image Quality Metrics:

IQM plays an important role in designing image processing algorithms. IQM may be used to measure the output of the processed image. Quality of image is defined as a function of an image which measures the image degradation processed by comparison with an optimized image. Subjective process measurement of image quality is known to be an accurate method [31]. The use of the subjective approach,is limited in real time implementations because of its complications and difficulties in its execution. In recent years, however, quantitative approaches have been more commonly used for the measurement of image quality.In this work, we discuss multiple measurements of image quality and assess their statistical actions for seven focused indicators of the SFF system.

1. Mean Squared Error (MSE)

MSE is a very easy and regular measure of distortion.The MSE between the referential image and the processed image $(x' \ y)$ is expressed as follows:

$$MSE = \frac{1}{xy} \sum_{i=1}^{x} \sum_{j=1}^{y} (A_{ij} - B_{ij})^2 \qquad (22)$$

where A_{ij} and B_{ij} are the reference image and processed image pixel values respectively.The MSE value calculates the difference between an image processed and the reference image.This increases the smaller value of the MSE.

2.Peak Signal to Noise Ratio (PSNR)

PSNR (Peak Signal to Noise Ratio) is one of the most widely used metric metrics for calculating the reconstruction efficiency. It represents the relationship between the maximal power of a signal and the power of corrupting sound and is typically seen in decibel size. The following can be said about PSNR:

$$PSNR(db) = 10\log \frac{255^2}{MSE} \qquad (23)$$

A higher PSNR value implies higher quality restoration.

3.Structural Content (SSIM)
The following is reflected in this quality metric:

$$\text{SSIM} = \frac{\sum_{i=1}^{x} \sum_{j=1}^{y} (A_{ij})^2}{\sum_{i=1}^{x} \sum_{j=1}^{y} (B_{ij})^2} \qquad (24)$$

A higher SC value indicates that the picture is of low quality.

4.Normalized Cross Correlation (NCC)
The measure NCC demonstrates the contrast ofthe picture processed with the reference picture.The following was represented by NCC:

$$\text{NCC} = \sum_{i=1}^{x} \sum_{j=1}^{y} \frac{(A_{ij}*B_{ij})}{A_{ij}^2} \qquad (25)$$

5.Maximum Difference (MD)
MD produces the highest error difference between the processed and reference image.The following aredescribed below,

$$MD = Max(|A_{ij} - B_{ij}|) \qquad (26)$$
$$i = 1,2,3,\text{L} \ x \& \ j = 1,2,3,\text{L} \ y$$

The maximum variationvalue, the lower the image quality.

6.Normalized Absolute Error (NAE)
TheNAE quality measure can be expressed as follows

$$NAE = \frac{\sum_{i=1}^{x} \sum_{j=1}^{y} (|A_{ij}-B_{ij}|)}{\sum_{i=1}^{x} \sum_{j=1}^{y} (A_{ij})} \qquad (27)$$

A higher NAE value reveals a low quality image,

7.Average Difference (AD)
The average differences for the processedand source image are made by AD.The following AD can be expressed:

$$AD = \frac{1}{xy} \sum_{i=1}^{x} \sum_{j=1}^{y} [A_{(i,j)} - B_{(i,j)}] \qquad (28)$$

It should ideally be zero.

IV. SIMULATION RESULTS AND ANLAYSIS

A database of first 3 MRI brain tumor images and the next database of 2 liver images are shown in Fig. 3(a).The collection was compiled with numerous complex images of brain tumors. These images have been obtained from the kaggle and pre-
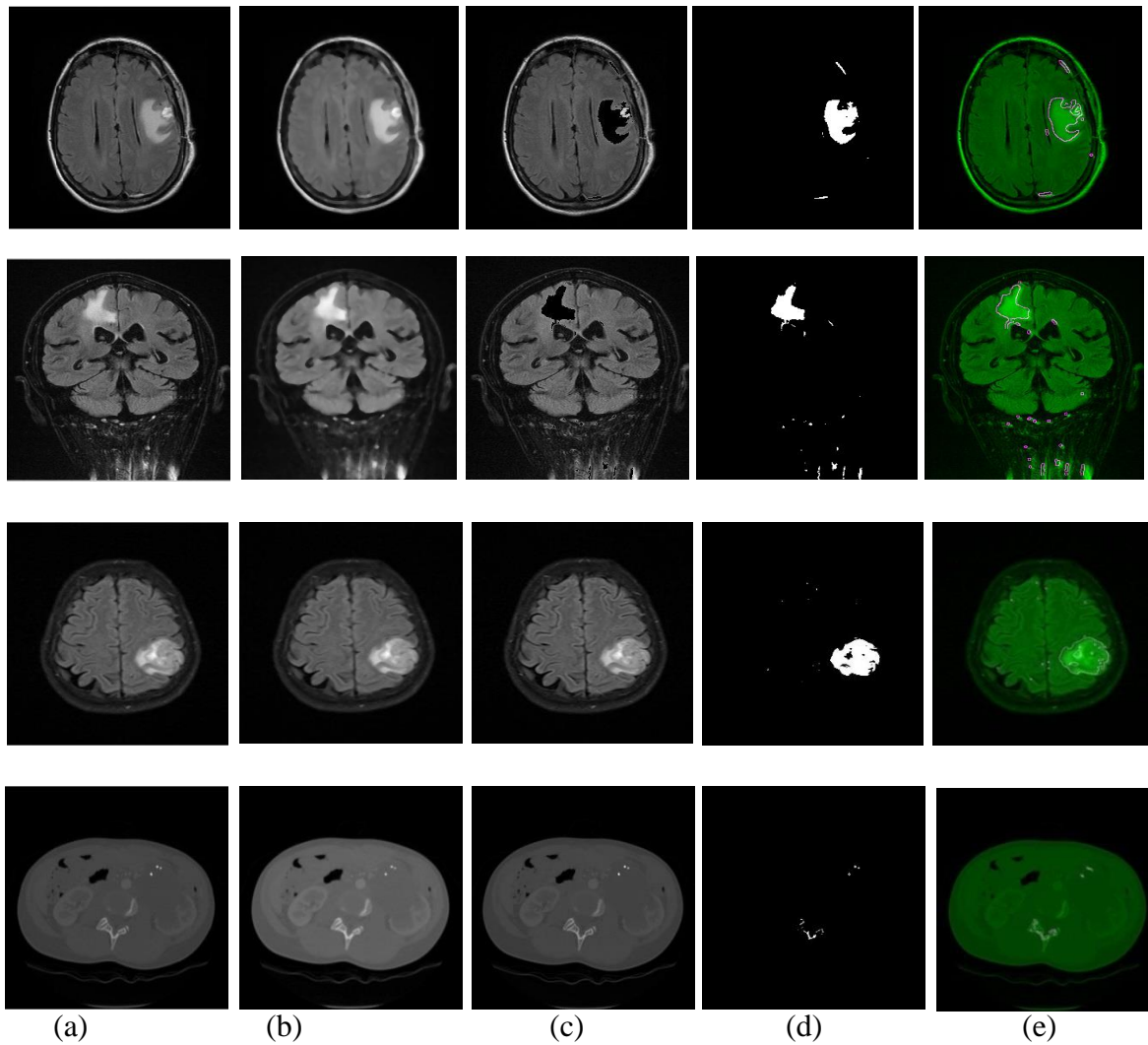
Fig. 3. Various images (a) Input MR images, (b) Pre-processed images, (c) ROI-based segmentation images, (d) FCM extracted tumor-affected area, (e) Area of the tumor-affected region.

Table 1. The performance analysis of segmented images with the calculation of area

Algorithms	**K-means**		**Fuzzy C-means**		**FCM Threshold**		**Kernel FCM**	
Images	I1_Brain1	I2_liver	I1_Brain1	I2_liver	I1_Brain1	I2_liver	I1_Brain1	I2_liver
Tumour Area	0.0204	0.0001	0.0125	0.0001	0.019	0.0013	0.0187	0.042
Number of Pixel	1619	35	992	37	1530	333	1486	1078
r_compression ratio	30.49	2004.1	50.87	1935.99	32.32	359.22	33.72	5292.
r_bits per pixel	0.2624	0.0040	0.1573	0.0041	0.2477	0.0223	0.2372	0.001
n_compression ratio	8.8359	14.310	8.7455	16.9773	8.9654	17.380	8.7465	21.46
n_bits per pixel	0.9054	0.5590	0.9148	0.4712	0.8923	0.4603	0.9147	0.372
Time	21.8758	70.432	21.8758	70.4322	21.8758	70.432	21.875	70.43

Processing is done in our algorithmic program for effective use. Then, by MATLAB 2014(a), we processed these original images and produced the final implementation database in figure 3. The tumors in such images have become so vital that they are too difficult to detect too easily by the ordinary people.

The preprocessing of MR images is very important for further processing to enhance the visual effect of an image. The captured images in the dataset are usually of such low quality that noise is removed and the image sharpened. The obtained image is preprocessed and converted into a 2-D matrix, and the RGB image converted into grey image. A median filter is used to extract the noise from the background. Then the image is changed with an optimized operation, a histogram dependent operation and a histogram-based adaptive operation. Improving an image usually requires enhancing the image contrast.

Initially, multiple attributes are indirectly extracted. Each part of the brain tumor should also not be avoided, including a small part of the brain tumor. The first step is to process the input image via Gaussian and Medium filters described in Figure 3. (b). Segmentation images from the region are illustrated in Figure 3 (c). The first segmentation of the image using Karinalized FCM (KFCM) template is then shown in Figure 3(d) based on its grey intensity and color temperature, where C=4 is segmented. The tumor is then filtered again through a median filter.So the tumor has been detected and represented red line using an enhanced FCM algorithm, which depends mainly on the Euclidean distance from the cluster centre to each data centre. This might be important in order to understand the significance of this modified and integrated technique. Finally, Figure 3(e) shows the area of the identified tumor.

Evaluation of output and segmented images The tumor extracted field estimation of trained MR images seen in table 1. The contrast between trained MR images was more evident from the observation than the tested MR images, while the homogeneity of trained MR images was lower than the tested MR images. In contrast to studied MR images, energy and homogeneity are even more found in qualified MR images. This proposed technique has been used to produce photographs of the brain tumor using mathematical structural information such as contrast, correlation, energy and homogeneity. The differences in statistical textural feature values of trained and tested brain tumors were found to be very useful in manipulating the performance of the KFCM in training and testing.

The MRI brain and liver image features were extracted successfully. The contrast and correlation ofbrain MR images were higher than those of liver MR images. However, the energy, homogeneity and correlation were higher in liver MR images than in brain MR images. Therefore, there were statistically significant differences in the variables of texture features is shown in Table 2. Thus, the heterogeneity or complexity of brain MR images was higher than those of liver MR images, while more homogenous and uniform appearances were observed for liver MR images.

The results of the applied target measures were analyzed with the image statistical metrics MSE, PSNR, NCC, AD, SSIM, MD and NAE. The results of the objective measurements measured statistically are described in table 3. In the absence of noise it contrasts and gives the ideal values of these metrics the different statistical metrics of the depth maps and all-in-center picture. Table 3 shows that Laplacian operators' statistical metrics are similar to the optimal values. With LAPD focus measurement, slightly improved outcomes are obtained.For instance, MSEis a basic and normal measure of distortion. The MSE value is the difference between the processed image and the reference image. Significantly higher MSE the outcome is much better. PSNR is also one of the most commonly used quality metrics for calculating the consistency of the reconstruction. A higher PSNR value implies a higher quality reconstruction.

V. CONCLUSIONS

This proposed work in this paper gives a higher result than traditional schemes of the proposed KFCM algorithm. This algorithm is often found to be optimal relative to standard systems. When the proposed KFCM algorithm detects human brain tumors, SSIMs are 35.1% and 34.89% above the FCM threshold, FCM and K-mean algorithms respectively. Furthermore, the PSNR of the KFCM algorithm is 11.04% more and the MSE among all the other algorithms is slightly smaller.Moreover, the tumor region of the proposed KFCM algorithm has been decreased by 3 percent and statistics for extracting energy and homogeneity nearly achieved by the value of one (1). However, with the proposed KFCM algorithm the time taken to diagnose the brain tumor is very limited than traditional algorithms.

Table 2. Statistical Features Analysis of segmented images

Algorithms	K-means		Fuzzy C-means		FCM Threshold		Kernel FCM	
Images	I1_Brain1	I2_liver	I1_Brain1	I2_liver	I1_Brain1	I2_liver	I1_Brain1	I2_liver

Contrast	0.1311	0.0035	0.1113	0.0035	0.1261	0.0322	0.1459	0
Correlation	0.9332	0.7428	0.9081	0.7567	0.9320	0.7474	0.9191	NaN
Energy	0.9573	0.9997	0.9730	0.9996	0.9596	0.9967	0.9602	1
Homogeneity	0.9977	0.9999	0.9980	0.9999	0.9977	0.9994	0.9974	1

Table 3. MR Image Quality Metrics

Algorithms	K-means		Fuzzy C-means		FCM Threshold		Kernel FCM	
Images	I1_Brain1	I2_liver	I1_Brain1	I2_liver	I1_Brain1	I2_liver	I1_Brain1	I2_liver
Mean Square Error	1352.1	2652.0	4593.02	2385.27	3997.7	1920.7	1322.05	134.67
Peak Signal to Noise Ratio	16.8207	13.895	11.5098	14.3554	12.112	15.296	16.9183	26.838
Normalized Cross-Correlation	0.7094	1.9301	1.2851	1.7092	1.1527	1.5914	0.8558	0.9756
Average Difference	2.5837	-32.97	-19.478	-22.026	-14.826	-18.48	2.4658	0.1020
Structural Content	0.5480	0.5833	0.5368	0.5945	0.6964	0.7367	0.9894	0.9932
Maximum Difference	227	229	247	229	247	229	227	104
Normalized Absolute Error	0.4032	1.0619	1.2032	0.9852	1.1155	0.8852	0.4310	0.0923

REFERENCES

[1] Lei, T., Jia, X., Zhang, Y., He, L., Meng, H., & Nandi, A. K. (2018). Significantly fast and robust fuzzy c-means clustering algorithm based on morphological reconstruction and membership filtering.IEEE Transactions on Fuzzy Systems, 26(5), 3027-3041.

[2]Stefanatos, R., &Sanz, A. (2018).The role of mitochondrial ROS in the aging brain.FEBS letters, 592(5), 743-758.

[3] Kanniappan, S., Samiayya, D., Vincent PM, D. R., Srinivasan, K., Jayakody, D. N. K., Reina, D. G., & Inoue, A. (2020). An Efficient Hybrid Fuzzy-Clustering Driven 3D-Modeling of Magnetic Resonance Imagery for Enhanced Brain Tumor Diagnosis.Electronics, 9(3), 475.

[4] Czajkowska, J., Kawa, J., Czajkowski, Z., &Grzegorzek, M. (2013, June). 4-D fuzzy connectedness-based medical image segmentation technique. In Proceedings of the 20th International Conference Mixed Design of Integrated Circuits and Systems-MIXDES 2013 (pp. 519-524). IEEE.

[5] Godinho, T. M., Lebre, R., Silva, L. B., & Costa, C. (2017). An efficient architecture to support digital pathology in standard medical imaging repositories.Journal of biomedical informatics, 71, 190-197.

[6] Alam, M. S., Rahman, M. M., Hossain, M. A., Islam, M. K., Ahmed, K. M., Ahmed, K. T., ...&Miah, M. S. (2019). Automatic human brain tumor detection in MRI image using template-based K means and improved fuzzy C means clustering algorithm. Big Data and Cognitive Computing, 3(2), 27.

[7] Joseph, R. P., Singh, C. S., &Manikandan, M. (2014). Brain tumor MRI image segmentation and detection in image processing.International Journal of Research in Engineering and Technology, 3(1), 1-5.

[8] Vishnuvarthanan, G., Rajasekaran, M. P., Subbaraj, P., &Vishnuvarthanan, A. (2016). An unsupervised learning method with a clustering approach for tumor identification and tissue segmentation in magnetic resonance brain images.Applied Soft Computing, 38, 190-212.

[9] Angulakshmi, M., & Lakshmi Priya, G. G. (2017). Automated brain tumour segmentation techniques—a review. International Journal of Imaging Systems and Technology, 27(1), 66-77.

[10] Al-Moteri, M. O., Symmons, M., Plummer, V., & Cooper, S. (2017). Eye tracking to investigate cue processing in medical decision-making: A scoping review. Computers in Human Behavior, 66, 52-66.

[11] Hunnur, S. S., Raut, A., &Kulkarni, S. (2017, July). Implementation of image processing for detection of brain tumors.In2017 International Conference on Computing Methodologies and Communication (ICCMC) (pp. 717-722).IEEE.

[12] Chanchlani, A., Chaudhari, M., Shewale, B., &Jha, A. (2017).Tumor detection in brain MRI using clustering and segmentation algorithm.IJARIIE-ISSN (O)-2395-4396, 3.

[13] Koundal, D., Kadyan, V., Dutta, P., Anand, V., Aggarwal, S., & Gupta, S. (2020). Computational techniques in biomedical image analysis: overview. Advances in Computational Techniques for Biomedical Image Analysis, 3-31.

[14] Vilela, P., & Rowley, H. A. (2017). Brain ischemia: CT and MRI techniques in acute ischemic stroke. European journal of radiology, 96, 162-172.

[15] Teichgraeber, H., & Brandt, A. R. (2019). Clustering methods to find representative periods for the optimization of energy systems: An initial framework and comparison.Applied energy, 239, 1283-1293.

[16] Lei, T., Jia, X., Zhang, Y., He, L., Meng, H., & Nandi, A. K. (2018). Significantly fast and robust fuzzy c-means clustering algorithm based on morphological reconstruction and membership filtering.IEEE Transactions on Fuzzy Systems, 26(5), 3027-3041.

[17] Nongmeikapam, K., Kumar, W. K., & Singh, A. D. (2017). Fast and automatically adjustable GRBF kernel based fuzzy C-means for cluster-wise coloured feature extraction and segmentation of MR images. IET image processing, 12(4), 513-524.

[18] Alagarsamy, S., Kamatchi, K., Govindaraj, V., Zhang, Y. D., &Thiyagarajan, A. (2019). Multi-channeled MR brain image segmentation: A new automated approach combining BAT and clustering technique for better identification of heterogeneous tumors. Biocybernetics and Biomedical Engineering, 39(4), 1005-1035.

[19] Sheela, C. J. J., &Suganthi, G. (2020). Morphological edge detection and brain tumor segmentation in Magnetic Resonance (MR) images based on region growing and performance evaluation of modified Fuzzy C-Means (FCM) algorithm.Multimedia Tools and Applications, 1-14.

[20] Khanmohammadi, S., Adibeig, N., &Shanehbandy, S. (2017). An improved overlapping k-means clustering method for medical applications.Expert Systems with Applications, 67, 12-18.

[21] Salem, S. B., Naouali, S., &Chtourou, Z. (2018). A fast and effective partitional clustering algorithm for large categorical datasets using a k-means based approach. Computers & Electrical Engineering, 68, 463-483.

[22] De Brabandere, B., Neven, D., & Van Gool, L. (2017).Semantic instance segmentation with a discriminative loss function.arXiv preprint arXiv:1708.02551.

[23] Mishro, P. K., Agrawal, S., Panda, R., & Abraham, A. (2020). A novel type-2 fuzzy C-means clustering for brain MR image segmentation.IEEE Transactions on Cybernetics.

[24] Guo, L., Chen, L., Chen, C. P., & Zhou, J. (2018). Integrating guided filter into fuzzy clustering for noisy image segmentation. Digital Signal Processing, 83, 235-248.

[25] Farahani, F. V., Ahmadi, A., &Zarandi, M. H. F. (2018). Hybrid intelligent approach for diagnosis of the lung nodule from CT images using spatial kernelized fuzzy c-means and ensemble learning. Mathematics and Computers in Simulation, 149, 48-68.

[26]Hu, G., & Du, Z. (2019). Adaptive kernel-based fuzzy c-means clustering with spatial constraints for image segmentation.International Journal of Pattern Recognition and Artificial Intelligence, 33(01), 1954003.

[27] Pham, T. X., Siarry, P., &Oulhadj, H. (2019). A multi-objective optimization approach for brain MRI segmentation using fuzzy entropy clustering and region-based active contour methods.Magnetic resonance imaging, 61, 41-65.

[28] Eresen, A., Birch, S. M., Alic, L., Griffin, J. F., Kornegay, J. N., &Ji, J. X. (2018). New similarity metric for registration of MRI to histology: Golden retriever muscular dystrophy imaging. IEEE Transactions on Biomedical Engineering, 66(5), 1222-1230.

[29] Khalifa, F., Soliman, A., Elmaghraby, A., Gimel'farb, G., & El-Baz, A. (2017). 3D kidney segmentation from abdominal images using spatial-appearance models.Computational and mathematical methods in medicine, 2017.

[30] Alharan, A. F., Fatlawi, H. K., & Ali, N. S. (2019). A cluster-based feature selection method for image texture classification.Indonesian Journal of Electrical Engineering and Computer Science, 14(3), 1433-1442.

[31] Kalaiselvi, T., &KarthigaiSelvi, S. (2018). Investigation of Image Processing Techniques in MRI Based Medical Image Analysis Methods and Validation Metrics for Brain Tumor. Current Medical Imaging, 14(4), 489-505.

***